Journal of Animal & Plant Sciences, 32(3): 2022, Page: 764-774
ISSN (print): 1018-7081; ISSN (online): 2309-8694
http://doi.org/10.36899/JAPS.2022.3.0478

CHARACTERIZING SILVER NANOPARTICLES BIOSYNTHESIZED FROM *SALVIA ROSMARINUS* AND ASSESSING THEIR *IN VITRO* ANTIFUNGAL AND CYTOTOXIC ACTIVITIES AGAINST PHYTOPATHOGENS AND CERVICAL CELLS

H. Rizwana*[1], N. A. Bokahri[1], S. A. Rashed[1], S. A. Shehri[1], M. A. Awad[2], N. Merghani [3] and H. Tabasuum[4]

[1]Department of Botany and Microbiology, College of Science, King Saud University, P. O Box 22452, Riyadh–11495, Kingdom of Saudi Arabia
[2]King Abdullah Institute for Nanotechnology, King Saud University, Riyadh 11451, Saudi Arabia.
[3] Central Laboratory, Female Center for Medical Studies and Scientific Section, King Saud University, Riyadh, KSA, Saudi Arabia
[4]Department of Clinical Laboratory Sciences, College of Applied Medical Science.
King Saud University, P. O. Box 22452, Riyadh-11495, Riyadh- Saudi Arabia
*For correspondence: hrizwana@ksu.edu.sa

ABSTRACT

Nanotechnology is significantly revolutionizing world agriculture through engineered nanomaterials, which contribute to enhancing agricultural production by controlling fungal and bacterial phytopathogens and, consequently, minimizing crop losses. In this study green silver nanoparticles (AgNPs) were biosynthesized using aqueous extracts of organically grown *Salvia rosmarinus* leaves.The AgNPs were examined and characterized with ultraviolet–visible spectroscopy, dynamic light scattering, energy-dispersive X-ray spectroscopy, transmission electron microscopy, and Fourier transform infrared spectroscopy. Their antifungal activity was evaluated against an array of fungal phytopathogens. In addition, the AgNPs were tested for their cytotoxic properties using microculture tetrazolium assays against the cervical cancer HeLa cell line. The nanoparticle size ranged between 7 and 58 nm, and the AgNPs significantly inhibited *Fusarium oxysporum* (61%), followed by *Alternaria alternata* (50%). The *in vitro* cytotoxicity assay against HeLa cells showed potent inhibition with a median inhibitory concentration of 11.28 ± 0.33 µg/mL. *S. rosmarinus* biosynthesized AgNPs demonstrate significant antifungal and antiproliferative activities against plant pathogens and HeLa cells.

Key words: *Salvia rosmarinus,* silver nanoparticles (AgNPs), phytopathogens, cytotoxicity

Published first online October 20. 2021 Published final May 30. 2022

INTRODUCTION

Plant pathogens in general and fungi in particular cause immense loss to plants by drastically lowering their yield, which affects the global economy. In addition, the quality of edible parts (fruits and vegetables) of plants is affected, raising serious concerns regarding human health. In the past few years, most agricultural research has aimed to increase the crop yield to meet the growing demands of the rising global population (Nellemann *et al*., 2009; Savary *et al*., 2012). Fungal pathogens, such as *Fusarium* spp., *Colletotrichum* spp., *Penicillium* spp., *Botrytis cinerea, Alternaria alternata,* and *Aspergillus* sp., cause many devastating postharvest diseases in fruits and vegetables, leading to a 25%–60% loss of total production (Gonzalez -Estrada *et al*., 2018). Postharvest spoilage due to fungi is predominantly controlled by applying chemical fungicides (Dukare *et al*., 2018). Although most fungicides are effective against fungal pathogens, their use is still questionable due to harmful effects on human health and the environment. Therefore, new eco-friendly biological fungicides that are less harmful to human health and the environment are required.

Nanotechnology is a novel technology that has opened new avenues and concepts that are applicable in various fields, such as medicine, pharmacology, chemistry, physics, and, recently, food sciences (Balaure *et al*., 2017; Sinha *et al*., 2017). Nanotechnology involves the synthesis and application of nanosized particles (1 - 100 nm), at this size, particles exhibit unique properties that are not present in their original form (Sandoval, 2009; Bajpai *et al*., 2018).). Many materials are used to prepare nanoparticles, such as metals and their oxides, lipids, emulsions, and ceramics. Recently, due to less toxicity and low cost, plants are also being explored extensively to prepare nanoparticles.

Silver nanoparticles (AgNPs) have drawn tremendous attention and increasing interest due to their high conductivity, catalytic activity, chemical stability, localized surface plasma resonance, and antimicrobial and anti-inflammatory activities (Ahmad *et al*., 2003; Ahmed *et al*., 2016). AgNPs are used for drug delivery, diagnosis, and tissue regeneration (Naidu *et al*., 2015); as postharvest/biological coatings (Balamurugan *et al*.,

2017) and antimicrobials (Qasim *et al*., 2018); and in the textile (Gokarneshan and Velumani, 2017), cosmetic (Naidu *et al*., 2015), and food (Carbone *et al*., 2016) industries.Green synthesis refers to the process of using plant extracts and microorganisms for nanoparticle synthesis. The various bioactive compounds in plants serve as reducing agents that render them safe and eco-friendly.

Salvia rosmarinus Spenn., commonly known as rosemary (*Rosmarinus officinalis* L), belongs to the Lamiaceae family and is a native of the Mediterranean region (de Macedo *et al*., 2020). It is an herb with fragrant leaves that are used in culinary settings as flavoring agents all over the world (Panda, 2009; Ibarra, 2010). *S. rosmarinus* has antiangiogenic (Kayashima and Matsubara, 2012), antibacterial (Georgantelis *et al*., 2007), and hepatoprotective properties (Raskovic *et al*., 2014). *S. rosmarinus* extracts have also shown anticancer properties against prostrate, colon, and skin cancer cell lines (Mirghaed and Yadollahi, 2013). In addition, the European Union has approved rosemary extracts (E3920 in EU additive regulation no. 1129/2011), and the European Food Safety Authority has proposed rosemary extracts as feed additives in the antioxidant class (Aguilar *et al*., 2008).

In this study, AgNPs were synthesized using aqueous leaf extracts of *S. rosmarinus* leaves, grown in an organic manner in Saudi Arabia. The biosynthesized AgNPs were characterized and evaluated for their cytotoxic and antifungal activities.

MATERIALS AND METHODS

Plant material and chemicals used: Fresh, disease free leaves of *S. rosmarinus* were provided by Dr. Sara Al Rashid and identified by plant taxonomist Professor Dr. Najat Al Bukhari. All the reagents used in the experimental work were of analytical grade and were obtained from Sigma-Aldrich.

Pathogens: *Alternaria. alternata*, *Fusarium solani*, *F. oxysporum*, *F. graminearum*, *Macrophomina phaseolina*, and *Trichoderma harzianum* were provided by the Department of Plant Protection at the College of Food and Agricultural Sciences, King Saud University, Riyadh, Saudi Arabia.

Preparation of aqueous leaf extracts: *S. rosmarinus* leaves were washed under running tap water to remove any adhering visible impurities and soil particles. The leaves were chopped and dried (25°C), and 10 g of roughly chopped leaves were added to a beaker containing 100 mL of distilled water. This mixture was heated at 60°C for 20 min. After cooling, the supernatant was filtered through Whatman filter paper (No. 1) and centrifuged at 5000 rpm for 5 min. The supernatant was collected and used to synthesize AgNPs.

Synthesis of green Ag nanoparticles: AgNP synthesis was performed as described by Jain and Mehata (2017) with slight modifications. Briefly, a fixed volume of $AgNO_3$ powder (0.0085 gm) was dissolved in 25 mL of distilled water to prepare 1 mM $AgNO_3$ solution. Next, 1 mL of aqueous leaf extract of *S. rosmarinus* was added to 5 mL of 1 mM $AgNO_3$ solution, mixed thoroughly on a magnetic stirrer, and observed for any color changes. A change in color from light yellow to colloidal brown indicated the formation of AgNPs. The biosynthesized AgNPs were assessed by ultraviolet–visible (UV–Vis) spectroscopy, field emission scanning electron microscopy (FE-SEM), dynamic light scattering (DLS), transmission electron microscopy (TEM), and Fourier transform infrared spectroscopy (FTIR).

Characterization of biosynthesized AgNPs

UV–Vis spectroscopy: V–Vis spectroscopy (Thermo Scientific 1500, USA) was performed on the biosynthesized AgNPs to assess the reduction of Ag^+ ions and the formation of AgNPs (colloidal-brown solution). The absorbance of the reaction mixture was measured at a wavelength of 200–700 nm.

Zetasizer: The biosynthesized AgNP samples were diluted with pure water, and the average size of the biosynthesized AgNPs was measured using a Nano–ZS-90 zetasizer (Malvern).

TEM: AgNP samples were prepared by carefully adding the biosynthesized AgNPs on a copper-coated grid. The average size of the AgNPs was determined by observing the samples under a JEM-1400 Plus transmission electron microscope (JEOL).

EDX analysis by scanning electron microscopy: The elemental composition (energy-dispersive X-ray spectroscopy [EDX]) of biosynthesized AgNPs was determined. A thin film of AgNPs was prepared on a glass slide by adding 8 µL of the suspension dropwise. The suspension was air-dried, coated with platinum, and observed by FE-SEM (JSM-7610F; JSM, Japan).

Fourier transform infrared spectroscopy (FTIR): The biomolecules present in the *S. rosmarinus* aqueous leaf extract and the biosynthesized AgNPs were analyzed by a Nicolet-6700 FTIR spectrometer (Thermo Scientific). The absorption spectrum was obtained at a scan range of 400–4000 cm^{-1} with a KBr pellet.

***In vitro* antifungal activity of the biosynthesized AgNPs:** The inhibitory activity of the biosynthesized AgNPs was tested against six phytopathogenic fungal strains. *In vitro* mycelial inhibition was tested using potato dextrose agar medium. Roughly, 15 mL of sterilized PDA was poured into a sterilized petri dish and allowed to solidify. Test fungi were separately grown in PDA plates for 5 days and later used to remove a 6 mm

mycelial plug for an *in vitro* assay. To test the effects of AgNPs on fungal growth, 1 mL of the biosynthesized AgNP suspension was added to sterile petri dishes, followed by 15 mL of PDA. The mixture was gently swirled and allowed to solidify. After solidification, the 6 mm mycelial plug removed from the periphery of test plates was placed in the center of the petri dishes in an upside-down manner. The dishes were incubated at 25°C ± 2°C for 7 days, and the diameter (mm) of the fungal colony was measured. Control dishes received only PDA (without AgNPs). The experiment was run in triplicate.

The effect of AgNPs on mycelial growth inhibition was calculated using the following formula:

Inhibition (%) = (Dfc − Dft)/Dfc × 100,

where Dfc is the average increase in mycelial growth in controls, Dft is the average increase in mycelial growth at each treatment.

Cytotoxicity (MTT assay): The cytotoxicity of the biosynthesized AgNPs was examined using 3-(4,5-dimethylthiazol-2-yl)-2, 5-diphenyltetrazolium bromide (MTT) assay, as described by Siddiqui *et al*. (2010). The human cervical cancer cell line (HeLa cells) was obtained from the American Type Culture Collection (USA). Briefly, HeLA cells were plated in 96-well plates at a density of 1×10^4 cells/well and allowed to settle for 24 h prior to treatment. The cells were treated with various concentrations of the biosynthesized AgNPs and prepared by twofold serial dilution. After incubating the plates for 24 h, MTT was added to the wells and the plates were further incubated for 4 h. Next, 200 µL of DMSO was added to the reaction mixture in each well and thoroughly mixed. All experiments were run in triplicate. Absorbance of the plates was measured at a wavelength of 550 nm, and the results were expressed as percentage cell viability. The median inhibitory concentration (IC50) was assessed using GraphPad Prism version 7, and a graph showing the dose-dependent response was generated using regression analysis.

RESULTS

Formation of *S. rosmarinus* AgNPs: Visual examination and UV–Vis spectral analysis: The formation of *S. rosmarinus* AgNPs was visually observed when the colorless $AgNO_3$ solution gradually transformed to a brown solution with an orange tint upon addition of the *S. rosmarinus* aqueous leaf extract. The color change indicated the formation of AgNPs due to surface plasmons. Fig. 1 shows the brown-colored solution, which indicates the formation of AgNPs. The process was gradual and started within the first few minutes of adding the *S. rosmarinus* aqueous leaf extract and took approximately 1 h to complete.

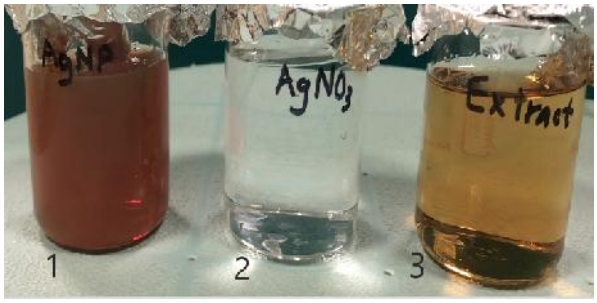

Figure 1. Visual examination of color changes during the biosynthesis of AgNPs from *Salvia rosmarinus* aqueous leaf extract. (1) Brown colloidal solution of biosynthesized AgNPs. (2) $AgNO_3$ solution. (3) Aqueous extract from fresh leaves.

The AgNP formation was further confirmed and measured with a UV–Vis spectrophotometer to obtain a surface plasmon resonance (SPR) band. The SPR band gradually increased in intensity for up to 50 min and then stopped after 1 h. The absorption band at 450 nm indicates the formation of AgNPs (Fig. 2).

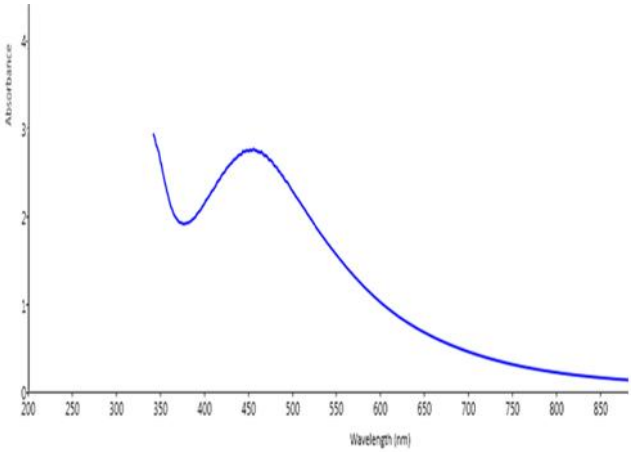

Figure 2. Absorption spectra of the AgNPs biosynthesized from *Salvia rosmarinus* aqueous leaf extracts.

Dynamic light scattering- particle size determination: The average size of the biosynthesized *S. rosmarinus* AgNPs was 56 nm, and the polydispersity index (PDI) was 0.285 (Fig. 3).

Transmission electron microscopy (TEM): Microphotographs showed uniform distribution of biosynthesized *S. rosmarinus* AgNPs. The particles were spherical in shape and separated in a uniform manner. The mean particle size was 7–58 nm (Fig. 4).

***Energy-dispersive spectrum (EDX)* of AgNPs:** EDX analysis of the biosynthesized *S. rosmarinus* AgNPs showed the presence of Ag, which is evident in the spectrum (Fig. 5). An absorption peak with an intense

signal was observed at 3 KeV, corresponding to the presence of AgNPs due to SPR. The presence of other elements was also observed in the spectrum.

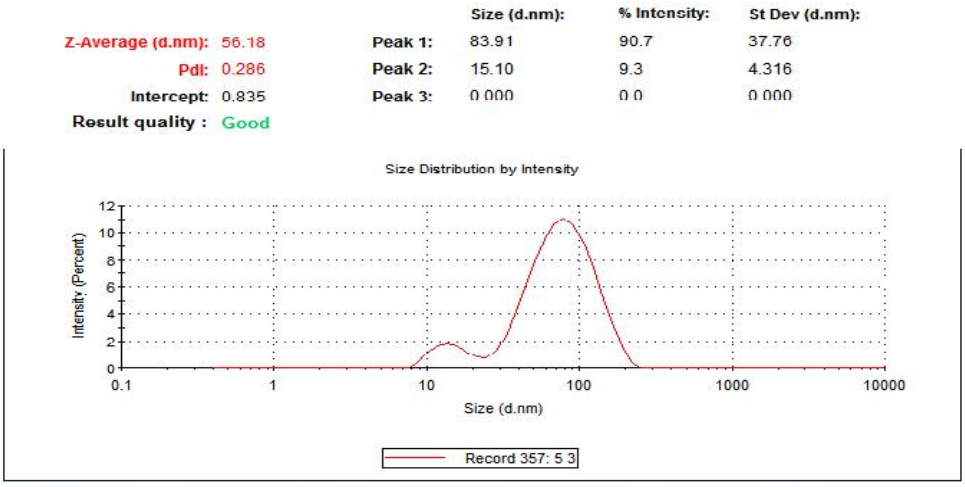

Figure 3. Average size measurements (diameter, nm) of AgNPs biosynthesized from *Salvia rosmarinus* aqueous leaf extracts.

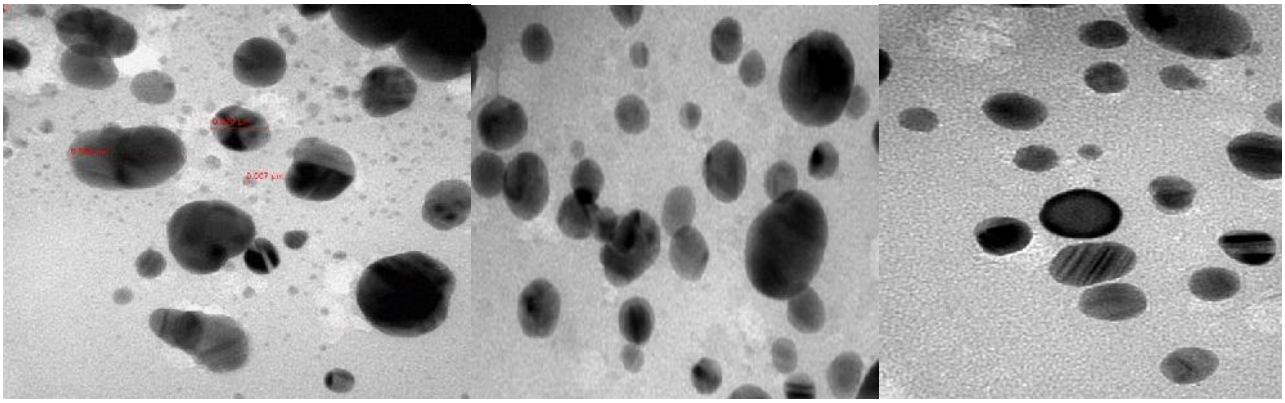

Figure 4. TEM microphotographs showing the size and morphology of AgNPs biosynthesized from *Salvia rosmarinus* aqueous leaf extracts.

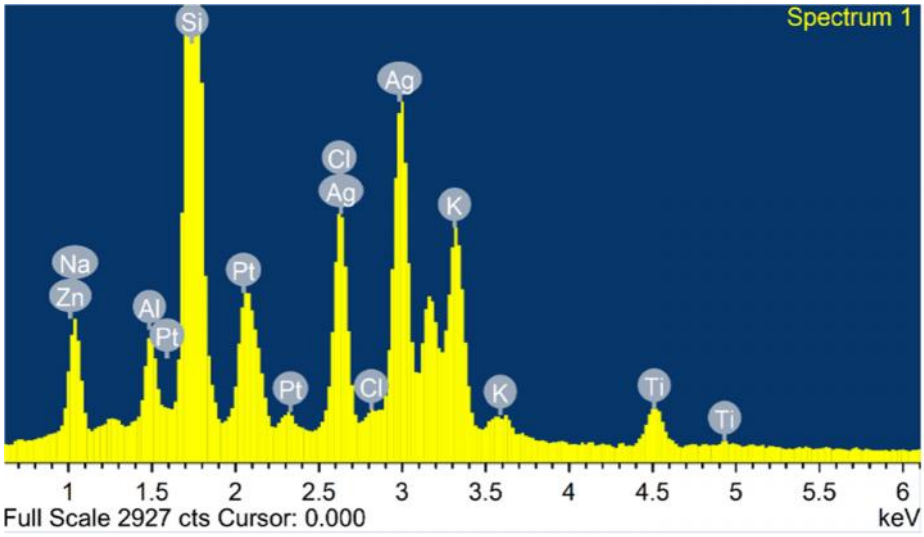

Figure 5. EDX spectrum of suspension of AgNPs biosynthesized from *Salvia rosmarinus* aqueous leaf extracts.

Fourier transform infrared spectroscopy (FTIR) of the extract and biosynthesized *S. rosmarinus* nanoparticles*:* The IR bands of both the *S. rosmarinus* aqueous leaf extract and synthesized *S. rosmarinus* AgNPs are shown in Fig. 6 and 7, respectively. Some common bands were observed in both spectra. The *S. rosmarinus* aqueous leaf extract revealed bands at 3402 cm^{-1} (corresponding to the O–H stretching of phenols) and 1605 cm^{-1} (corresponding to the C=C stretching of conjugated alkene). In addition, the 2 peaks at 1267 and 1039 cm^{-1} were due to C–O stretching. However, the IR spectrum of the *S. rosmarinus* AgNPs exhibited the disappearance of certain bands at 1524 (N–O stretching), 1405 (N–H bending vibration), and 813 cm^{-1} (C–H bending vibration), which were quite evident in the IR spectrum of the *S. rosmarinus* aqueous leaf extract. New peaks were also observed at 2928 and 1386 cm^{-1} in the spectrum of biosynthesized AgNPs. In addition, peaks of the *S. rosmarinus* aqueous leaf extract shifted from 3402, 1605, and 1386 cm^{-1} to 3426, 1620, and 1068 cm^{-1}, respectively, in the biosynthesized AgNPs and were tremendously narrower with weak transmittance (less intense).

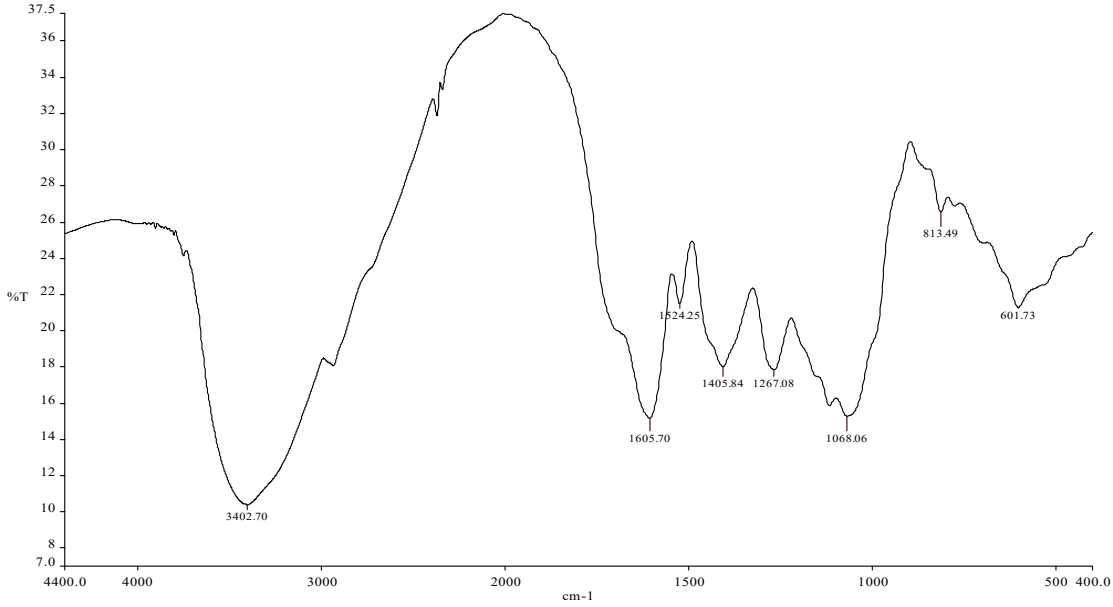

Figure 6. FTIR spectra of *Salvia rosmarinus* aqueous leaf extracts.

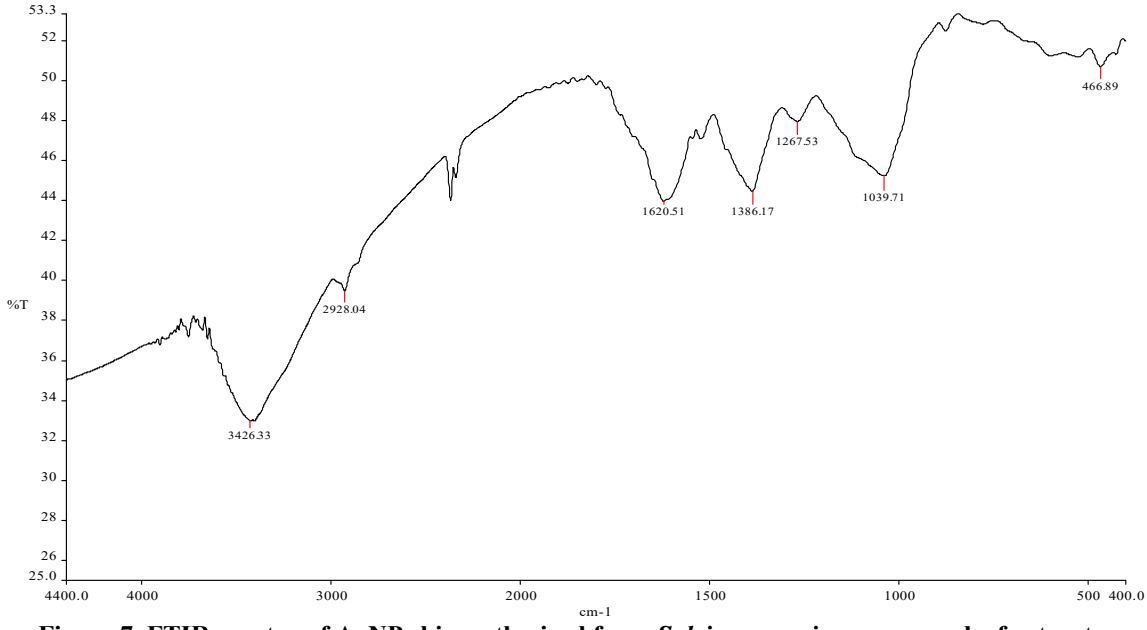

Figure 7. FTIR spectra of AgNPs biosynthesized from *Salvia rosmarinus* aqueous leaf extracts.

Antifungal activity: The biosynthesized AgNPs exhibited variable antifungal activity against phytopathogenic fungi. The highest antifungal activity was seen against *F. oxysporum*, followed by *A. alternata* and *F. solani* (61%, 50%, and 43%, respectively). However, poor mycelial inhibition was observed in other fungal strains (Fig. 8 and 9).

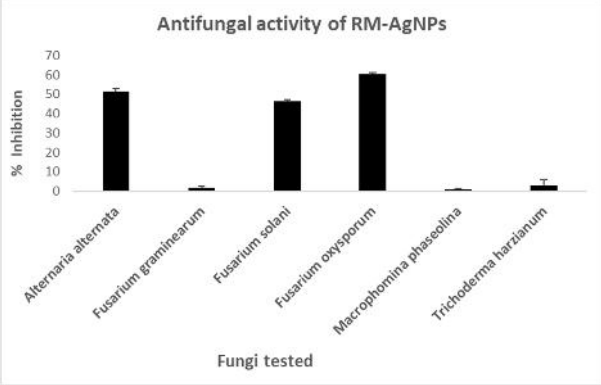

Figure 8. Antifungal activity of AgNPs biosynthesized from *Salvia rosmarinus* aqueous leaf extracts. AgNPs, silver nanoparticles.

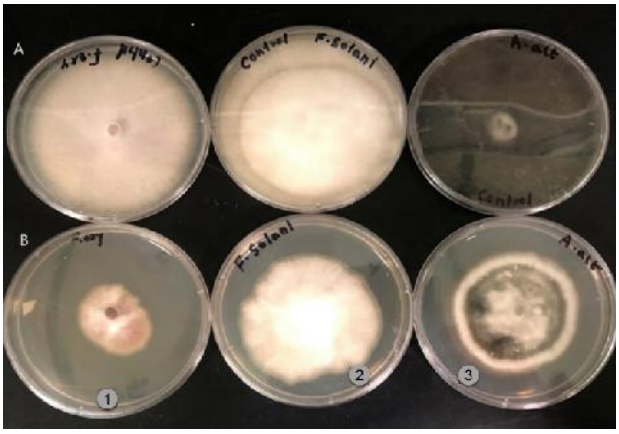

Figure 9. *In vitro* mycelial inhibition of phytopathogens treated with AgNPs biosynthesized from *Salvia rosmarinus* aqueous leaf extracts. (A) Fungal cultures not treated with biosynthesized AgNPs (control). (B) Fungi treated with biosynthesized AgNPs: 1, *Fusarium oxysporum*; 2, *F. solani*; and 3, *Alternaria alternata*. AgNPs, silver nanoparticles.

Cytotoxicity of AgNPs by MTT assay: To determine the *in vitro* cytotoxic activity of the biosynthesized AgNPs, MTT assay was performed. HeLA cells were treated with different concentrations (3.125–100 µg/mL) of biosynthesized AgNPs, as previously described. Fig. 10 shows the percentage growth inhibition of HeLa cells and their viability when treated with biosynthesized AgNPs compared to control cells (untreated). The cancer cell inhibition was dose dependent: cell viability decreased with an increase in the AgNP concentration. Significant inhibition began at a concentration of 25 µg/mL, as only 19% of HeLa cells were viable, which dropped to a maximum of 5% cell viability at 100 µg/mL. The IC50 value was 11.28 ± 0.33 µg/mL.

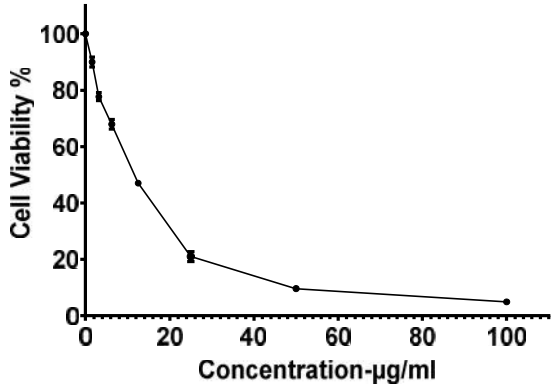

Figure 10. Cytotoxicity evaluation of AgNPs biosynthesized from *Salvia rosmarinus* aqueous leaf extracts against HeLA cells. AgNPs, silver nanoparticles.

DISCUSSION

This study demonstrated AgNP synthesis from *S. rosmarinus* aqueous leaf extracts. The appearance of a brown color marks the bioreduction of silver ions to AgNPs, while the UV–Vis spectrophotometer monitors the bioreduction process through the formation of a characteristic SPR peak. AgNPs show potent SPR activity in aqueous solutions (Shanker *et al*., 2004). The biosynthesized AgNPs showed an SPR peak at 450 nm, which was broad and pronounced, indicating that the AgNPs were polydispersed in nature. Characteristic AgNP peaks (λmax) are observed between 400 and 500 nm (Sastry *et al*., 1997). The absorption spectrum of AgNPs is highly sensitive to several factors (Jain and Mehata, 2017). The SPR position, shape, and size are affected by the dielectric medium, the size and shape of AgNPs, and the surroundings medium (Kelly *et al*., 2003; Zhao *et al*., 2008; Wani *et al*., 2010; Dada *et al*., 2017). *S. rosmarinus* aqueous leaf extracts contain phenolic compounds, flavonoids, and amides, which are responsible for the bioreduction of silver ions to AgNPs. Similar findings related to the SPR peak from *S. rosmarinus* AgNPs have also been previously reported (Ghaedi *et al*., 2015).

DLS analysis of the biosynthesized *S. rosmarinus* AgNPs showed that the PDI and average size of AgNPs were 56 and 0.28 nm, respectively, indicating that the *S. rosmarinus* AgNPs are stable. PDI values greater than 0.7 indicate that the sample has a broad size

(Roy *et al*., 2017). Since the PDI was lower than 0.7 in this study, the biosynthesized AgNPs are of considerably good quality. Our findings agree with those of previous reports in which PDI values of 0.398 and 0.7, respectively, were observed, since the plant extracts formed a wide range of coatings around the nanoparticles (De Aragao *et al*., 2016; Roy *et al*., 2017).

TEM microphotographs showed that the biosynthesized *S. rosmarinus* AgNPs were roughly spherical. The average size was 7–58 nm. In addition, the AgNPs were polydispersed, well separated, and distributed in a uniform manner. Their small size observed in the TEM microphotographs, in comparison to the DLS spectrum, is due to the physical state in which the sample was measured. As TEM requires dry samples (nanoparticles) and DLS requires hydrated particles, the hydrodynamic volume is larger in the hydrated state, which contributes to a large size of the nanoparticles (Gao *et al*., 2008). Biomolecules that are present in the *S. rosmarinus* leaf extract (aqueous) also caused capping of the AgNPs, which is evident in the microphotographs. Similar findings were previously reported in which various organic bioactive compounds present in plant extracts formed a thin coating around the nanoparticles, facilitated bioreduction, stabilized the biosynthesized nanoparticles, and sometimes also resulted in the agglomeration of a few nanoparticles (Mallikarjuna *et al*., 2014; Aritonang *et al*., 2019).

The EDX spectrum of the *S. rosmarinus* AgNPs showed a prominent peak at 3 KeV which indicates the presence of silver. The peak in this region is attributed to SPR, which ascertains AgNP formation (Das *et al*., 2013; Mallikarjuna *et al*., 2014). Besides, the silver peak, peaks related to other elements were also observed in the spectrum. These peaks arise due to elements that are present in the leaf extracts. The platinum peak is due to the coating used on the sample.

FTIR analysis was used to identify the potential biomolecules responsible for bioreduction and capping of silver ions during AgNP synthesis. The broad peaks in the *S. rosmarinus* aqueous leaf extract spectrum at 3402 cm^{-1} indicated that the extract was rich in phenols. However, after AgNP synthesis, the disappearance and narrowing of the certain peaks in the IR spectrum indicated that the biomolecules (functional groups) served a purpose in the bioreduction and synthesis of *S. rosmarinus* AgNPs. In addition, comparison of the IR spectra of biosynthesized *S. rosmarinus* AgNPs and leaf extract showed that several peaks observed in the leaf extract were shifted in the IR spectrum of synthesized AgNPs. Shifts in peaks from 1461 to 1386 cm^{-1} and from 3402 to 3426 cm^{-1}, suggests the involvement of bending vibration of N–H (amines) or alcoholic groups in Ag reduction. The peak at 1405 cm^{-1}, due to N–H bending in the amine group in the *S. rosmarinus* aqueous leaf extract, serves as a capping and stabilizing agent, as previously reported by Jyoti *et al*. (2016). Thus, FTIR analysis of biosynthesized AgNPs in this study evidently indicates the presence of phenols, aliphatic amines, terpenoids, and flavonoids. These molecules seem to surround the AgNPs and serve as strong binding sites for the AgNPs during synthesis. *S. rosmarinus* leaf extracts are rich in important secondary metabolites, such as flavonoids, phenols and carnosol derivatives, which play a key role in capping, reduction, and in providing stability (Shah *et al*., 2014). Previous studies suggest that the presence of functional groups on the surfaces of biosynthesized AgNPs are from *S. rosmarinus* aqueous leaf extracts and other plants (Fierascu *et al*., 2014; Prasannaraj and Venkatachalam, 2017; Femi-Adepoju *et al*., 2019).

AgNPs biosynthesized from *S. rosmarinus* aqueous leaf extracts show significant antifungal activity against phytopathogenic fungi but in a variable manner. The potent antifungal activity of certain biosynthesized nanoparticles has been previously reported (Gupta *et al*., 2014; Bahrami-Teimoori *et al*., 2017; Al-Zubaidi *et al*., 2019). The exact mode of action of AgNPs as antifungals is unclear. However, studies have shown that AgNPs adhere to fungal hyphae and conidia and potentially penetrate the cell membrane, which disrupts cell integrity (Srikar *et al*., 2016). Another perspective regarding significant antifungal activity involves interference with ergosterol synthesis, which directly affects the integrity of cell structures and leads to cell death (Radhakrishnan *et al*., 2018; Roy *et al*., 2019). In addition, the large surface area of AgNPs induces increased reactive oxygen species (ROS) and free-radical production and the leakage of DNA and proteins, resulting in cellular damage (Ogar *et al*., 2015; Dakal *et al*., 2016; Ibrahim *et al*., 2020). Previous studies have shown strong in vitro inhibition of fungi, such as *Bipolaris sorokiniana*, *Magnaporthe grisea*, and *Rhizoctonia solani*, when treated with nanoparticles biosynthesized from plants (Elgorban *et al*., 2016; Lopez *et al*., 2018). Recently, the in vitro inhibition of *Aspergillus oryzae* and *C. albicans* by *Rosmarinus officinalis* AgNPs was reported (Ghaedi *et al*., 2015).

Our findings showed potent cytotoxic activity of *S. rosmarinus* AgNP against HeLa cells, which could be due to the diverse bioactive compounds attached to the AgNPs and the nanosize that enables effective cell penetration. AgNPs induce cytotoxicity by disturbing the cell cycle of cancer cells and inhibiting cell proliferation (Dziedzic *et al*., 2016). A micronucleus (MN) assay recently revealed the genotoxic potential of AgNPs as they induced chromosomal damage and abnormalities during mitosis (Sahu *et al*., 2016). Biosynthesized nanoparticles cause HeLa cells to shrink, decrease in density, and lose cell adhesion capability (Al Sheddi *et al*., 2018). Similar dose-dependent cytotoxic effects and cellular changes have been reported for *S. rosmarinus*

AgNPs and some other green AgNPs against various cancer cell lines (Vivek *et al*., 2012; Sulaiman *et al*., 2013; Suman *et al*., 2013; Al Sheddi *et al*., 2018. Thus, the antiproliferative activity of *S. rosmarinus* AgNPs could be due to their capability to induce ROS generation and apoptosis (Stroh *et al*., 2004; Farah *et al*., 2016).

S. rosmarinus is a rich source of carnosol, carnosic acid, and rosmarinic acid. The two major components of rosemarinic acid and carnosic acid reportedly induce high cytotoxicity in breast cancer cell lines at an IC50 of 24.08–31.87 and 12.50 µg/mL, respectively (Yesil-Celiktas *et al*., 2010). *S. rosmarinus* aqueous leaf extracts and carnosic acid exert antitumorigenic effects and promote apoptosis (Huang *et al*., 1994; Petiwala *et al*., 2013). Our findings are consistent with all previous studies, as the *S. rosmarinus* aqueous leaf extracts have demonstrated significant antiproliferative activity against several human cancer cell lines.

Conclusion: The biosynthesized AgNPs demonstrated significant antifungal and antiproliferative activities against plant pathogens and HeLa cells. Based on the findings of this study, AgNPs synthesized from *S. rosmarinus* leaf extracts can be applied in postharvest technology and for crop protection against harmful fungal pathogens. In addition, *S. rosmarinus* AgNPs can be further explored for their anticancer properties against various cancer cell lines.

Acknowledgments: This study was supported by a grant from the Researchers Support Project. The authors would like to extend their sincere appreciation to the Researchers Supporting Project (number: RSP-2021/229), King Saud University, Riyadh, Saudi Arabia for the funding of this work.

REFERENCES

Aguilar, F., H. Autrup, S. Barlow, L. Castle, R. Crebelli, W. Dekant, K.H. Engel, N. Gontard, D. Gott and S. Grilli (2008). Use of rosemary extracts as a food additive-scientific opinion of the panel on food additives, flavourings, processing aids and materials in contact with food. EFSA. J. 721: 1-29.

Ahmad, A., P. Mukherjee, S. Senapati, D. Mandal, M.I. Khan, R. Kumar and M. Sastry (2003). Extracellular biosynthesis of silver nanoparticles using the fungus *Fusarium oxysporum.* Colloids Surf. B. 28(4): 313-318.

Ahmed, S., M. Ahmad, B.L. Swami and S. Ikram (2016). A review on plants extract mediated synthesis of silver nanoparticles for antimicrobial applications: a green expertise. J. Adv. Res. 7(1): 17-28.

Al-Sheddi, E.S., N.N. Farshori, M.M. Al-Oqail, S.M. Al-Massarani, Q. Saquib, R. Wahab, J. Musarrat, A.A. Al-Khedhairy and M.A. Siddiqui (2018). Anticancer potential of green synthesized silver nanoparticles using extract of *Nepeta deflersiana* against human cervical cancer cells (HeLA). Bioinorg. Chem. Appl. Article ID 9390784, 12 pages, 2018. https://doi.org/10.1155/2018/9390784

Al-Zubaidi, S., A. Al-Ayafi and H. Abdelkader (2019). Biosynthesis, characterization, and antifungal activity of silver nanoparticles by *Aspergillus niger* isolate. J. Nanotechnol. Res. 1(1): 23-36.

Aritonang, H.F., H. Koleangan and A.D. Wuntu (2019). Synthesis of silver nanoparticles using aqueous extract of medicinal plants' (*Impatiens balsamina* and *Lantana camara*): fresh leaves and analysis of antimicrobial activity. Int. J. Microbiol. :8642303. 8 pages, doi: 10.1155/2019/8642303. PMID: 31354833; PMCID: PMC6636566.

Bahrami-Teimoori, B., Y. Nikparast, M. Hojatianfar, M. Akhlaghi, R. Ghorbani and H.R. Pourianfar (2017). Characterisation and antifungal activity of silver nanoparticles biologically synthesized by *Amaranthus retroflexus* leaf extract. J. Exp. Nanosci. 12(1): 129-139.

Bajpai, V.K., M. Kamle, S. Shukla, D.K. Mahato, P. Chandra, S.K. Hwang, P. Kumar, Y.S. Huh and Y.K. Han (2018). Prospects of using nanotechnology for food preservation, safety, and security. J. Food Drug Anal. 26(4): 1201-1214.

Balamurugan, M., S. Saravanan and T. Soga (2017). Coating of green-synthesized silver NPs on cotton fabric. J. Coat. Technol. Res. 14(3): 735-745.

Balaure, P.C., D. Gudovan and I. Gudovan (2017). Nanopesticides: a new paradigm in crop protection. New Pestic. Soil Sens. 129-192.

Carbone, M., D.T. Donia, G. Sabbatella and R. Antiochia (2016). Silver NPs in polymeric matrices for fresh food packaging. J. King Saud Univ. Sci. 28(4): 273-279.

Dada, A.O., O.J. Ojediran, F.E. Dada, A.P. Olalekan and O.J. Awakan (2017). Green synthesis and characterization of silver nanoparticles using Calotropis procera extract. J. Appl. Chem. Sci. Int. 8(4): 137-143.

Dakal, T.C., A. Kumar, R.S. Majumdar and V. Yadav (2016). Mechanistic basis of antimicrobial actions of silver nanoparticles. Front. Microbiol. 7: 1831.

Das, J., M.P. Das and P. Velusamy (2013). Sesbania grandiflora leaf extract mediated green synthesis of antibacterial silver nanoparticles against

selected human pathogens. Spectrochim. Acta Part A. 104: 265-270.

de Aragao, A.P., T.M. de Oliveira, P.V. Quelemes, M.L.G. Perfeito, M.C. Araujo, J.D.A.S. Santiago and D.A. da Silva (2016). Green synthesis of silver nanoparticles using the seaweed Gracilaria birdiae and their antibacterial activity. Arab. J. Chem. 12(8): 4182-4188.

de Macedo L.M., É.M.D. Santos., L. Militão, L.L. Tundisi., J.A. Ataide., E.B. Souto., P.G. Mazzola(2020). Rosemary (Rosmarinus officinalis L., syn Salvia rosmarinus Spenn.) and Its Topical Applications: A Review. Plants (Basel).21;9 (5):651. doi: 10.3390/plants9050651. PMID: 32455585; PMCID: PMC7284349.

Dukare A.S., S. Paul, V. E. Nambi, R.K. Gupta, R. Singh, K. Sharma and R. K. Vishwakarma (2018) Exploitation of microbial antagonists for the control of postharvest diseases of fruits: a review, Critical Rev. Food. Sci. Nutr. DOI: 10.1080/10408398.2017.1417235

Dziedzic, A., R. Kubina, R.J. Buldak, M. Skonieczna and K. Cholewa (2016). Silver nanoparticles exhibit the dose-dependent anti-proliferative effect against human squamous carcinoma cells attenuated in the presence of berberine. Mol. 21(3): 365.

Elgorban, A.M., A.E.R.M. El-Samawaty, M.A. Yassin, S.R. Sayed, S.F. Adil, K.M. Elhindi, M. Bakri and M. Khan (2016). Antifungal silver nanoparticles: synthesis, characterization and biological evaluation. Biotechnol. Biotechnol. Equip. 30(1): 56-62.

Farah, M.A., M.A. Ali, S.M. Chen, Y. Li, F.M. Al-Hemaid, F.M. Abou-Tarboush, K.M. Al-Anazi and J. Lee (2016). Silver nanoparticles synthesized from *Adenium obesum* leaf extract induced DNA damage, apoptosis and autophagy via generation of reactive oxygen species. Colloids Surf. B 141: 158-169.

Femi-Adepoju, A.G., A.O. Dada, K.O. Otum, A.O. Adepoju, O.P. Fatoba (2019). Green synthesis of silver nanoparticles using terrestrial fern (Gleichenia pectinata (Willd.) C. Presl.): characterization and antimicrobial studies. Heliyon. 5(4): e01543.

Fierascu, R.C., I.R. Bunghez, R. Somoghi, I. Fierascu and R.M. Ion (2014). Characterization of silver nanoparticles obtained by using Rosmarinus officinalis extract and their antioxidant activity. Rev. Roum. Chim. 59(3-4): 213-218.

Gao, F.P., H.Z. Zhang, L.R. Liu, Y.S. Wang, Q. Jiang, X.D. Yang and Q.Q. Zhang (2008). Preparation and physicochemical characteristics of self-assembled nanoparticles of deoxycholic acid modified-carboxymethyl curdlan conjugates. Carbohydr. Polym. 71(4): 606-613.

Georgantelis, D., I. Ambrosiadis, P. Katikou, G. Blekas and S.A. Georgakis (2007). Effect of rosemary extract, chitosan and a-tocopherol on microbiological parameters and lipid oxidation of fresh pork sausages stored at 4°C. Meat Sci. 76(1): 172-181.

Ghaedi, M., M. Yousefinejad, M. Safarpoor, H. Zare Khafri and M.K. Purkait (2015). Rosmarinus officinalis leaf extract mediated green synthesis of silver nanoparticles and investigation of its antimicrobial properties. J. Ind. Eng. Chem. 31: 167-172.

Gokarneshan, N. and K. Velumani (2017). Application of nano silver particles on textile materials for improvement of antibacterial finishes. Global J. Pharm. Sci. 2: 1-4.

Gonzalez-Estrada, R., F. Blancas-Benitez, B. Montano-Leyva, C. Moreno-Hernandez, L.D.C. Romero-Islas, J. Romero-Islas, R. Avila-Penna, A. Ramos-Guerrero, A. Fonseca-Cantabrana and P. Gutierrez-Martinez (2018). A review study on the postharvest decay control of fruit by trichoderma. IntechOpen,10.5772/82784. Available from: https://www.intechopen.com/online-first/a-review-study-on-the-postharvest-decay-control-of-fruit-by-trichoderma

Gupta, A., A. Ingle, A.K. Gade, S. Gaikwad, M. Rai and S.R. Bonde (2014). Lawsonia inermis-mediated synthesis of silver nanoparticles: activity against human pathogenic fungi and bacteria with special reference to formulation of an antimicrobial nanogel. IET Nanobiotechnol. 8(3): 172-178.

Huang, M.T., C.T. Ho, Z. Wang, T. Ferraro, Y.R. Luo, K. Stauber, W. Ma, C. Georgiadis, J.D. Laskin and A.H. Conney (1994). Inhibition of skin tumorigenesis by rosemary and its constituents carnosol and ursolic acid. Cancer Res. 54(3): 701-708.

Ibarra, A., J. Cases, A. Bily, K. He, N. Bai, M. Roller, A. Coussaert and C. Ripoll (2010). Importance of extract standardization and /assay selection for the evaluation of antioxidant activity of botanicals: a case study on three Rosmarinus officinalis L extracts. J. Med. Food. 13(5): 1167-1175.

Ibrahim, E., M. Zhang, Y. Zhang, A. Hossain, W. Qiu, Y. Chen, Y. Wang, W. Wu, G. Sun and B. Li (2020). Green-synthesization of silver nanoparticles using endophytic bacteria isolated from garlic and its antifungal activity against wheat Fusarium head blight pathogen Fusarium graminearum. Nanomater. 10(2): 219.

Jain, S. and M.S. Mehata (2017). Medicinal plant leaf extract and pure flavonoid mediated green synthesis of silver nanoparticles and their enhanced antibacterial property. Sci. Rep. 7(1): 15867.

Jyoti, M., M. Baunthiyal and A. Singh (2016). Characterization of silver nanoparticles synthesized using Urticadioica Linn. leaves and their synergistic effects with antibiotics. J. Radiation Res. Appl. Sci. 9(3): 217-227.

Kayashima, T. and K. Matsubara (2012). Antiangiogenic effect of carnosic acid and carnosol, neuroprotective compounds in rosemary leaves. Biosci. Biotechnol. Biochem. 76: 115-119.

Kelly, K.L., E. Coronado, L.L. Zhao and G.C. Schatz (2003). The optical properties of metal nano particles: the influence of size, shape and dielectric environment. J. Phys. Chem. 107(3): 668-677.

Lopes, L.C.S., L.M. Brito, T.T. Bezerra, K.N. Gomes, F.A.D.A. Carvalho, M.H. Chaves and W. Cantanhêde (2018). Silver and gold nanoparticles from tannic acid: synthesis, characterization and evaluation of antileishmanial and cytotoxic activities. An. Acad. Bras. Cienc. 90(3): 2679-2689.

Mallikarjuna, K., N.J. Sushmab and G. Narasimhac (2014). Phytochemical fabrication and characterization of silver nanoparticles by using pepper leaf broth. Arab. J. Chem. 7(6): 1099-1103.

Mirghaed, A. and F. Yadollahi (2013). Evaluation of the chemical composition and in vitro antimicrobial activity of Rosmarinus officinalis, Zataria multiflora, Anethum graveolens and Eucalyptus globulus against Streptococcus iniae; the cause of zoonotic disease in farmed fish. Iran. J. Fish. Sci. 12(3): 702-716.

Naidu, K.S., P. Govender and J.K. Adam (2015). Nano silver particles in biomedical and clinical applications. Med. Technol. 29(2): 13-19.

Nellemann, C., M. MacDevett, T. Manders, B. Eickhout, B. Svilhus, A.G. Prins and B.P. Kaltenborn (2009). The environmental food crisis - the environment's role in averting future food crises. A UNEP rapid response assessment. United Nations Environment Program, GRID-Arendal, Pg-1-104 .www.grida.no ISBN: 978-82-7701-054-0

Ogar, A., G. Tylko and K. Turnau (2015). Antifungal properties of silver nanoparticles against indoor mould growth. Sci. Total Environ. 521-522: 305-314.

Panda, H. (2009). Cultivation of in aromatic plants cultivation, processing and uses. National Institute of Industrial Research. Asia Pacific Business Press, Inc., New Delhi, India.

Petiwala, S.M., A.G. Puthenveetil and J.J. Johnson (2013). Polyphenols from the Mediterranean herb rosemary (*Rosmarinus officinalis*) for prostate cancer. Front. Pharmacol. 4: 29.

Prasannaraj, G. and P. Venkatachalam (2017). Green engineering of biomolecule-coated metallic silver nanoparticles and their potential cytotoxic activity against cancer cell lines. Adv. Nat. Sci. Nanosci. Nanotechnol. 8(2): 025001.

Qasim, M., N. Udomluck, J. Chang, H. Park and K. Kim (2018). Antimicrobial activity of silver NPs encapsulated in polyN-isopropylacrylamide-based polymeric NPs. Int. J. Nanomed. 13: 235.

Radhakrishnan, V.S., M.K. Reddy, M. Kumar, S.P. Dwivedi, S.P. Singh, T. Prasad (2018). Silver nanoparticles induced alterations in multiple cellular targets, which are critical for drug susceptibilities and pathogenicity in fungal pathogen (*Candida albicans*). Int. J. Nanomed. 13: 2647-2663.

Raškovic, A., I. Milanovic, N. Pavlovic, T. Cebovic, S. Vukmirovic and M. Mikov (2014). Antioxidant activity of rosemary (*Rosmarinus officinalis* L.) essential oil and its hepatoprotective potential. BMC Complement. Altern. Med. 14: 225.

Roy, A., O. Bulut, S. Some, A.K. Mandal and M.D. Yilmaz (2019). Green synthesis of silver nanoparticles: biomolecule-nanoparticle organizations targeting antimicrobial activity. RSC Adv. 9(5): 2673.

Roy, P., B. Das, A. Mohanty and S. Mohapatra (2017). Green synthesis of silver nanoparticles using Azadirachta indica leaf extract and its antimicrobial study. Appl. Nanosci. 7(8): 843-850.

Sahu, S.C., S. Roy, J. Zheng and J. Ihrie (2016). Contribution of ionic silver to genotoxic potential of nanosilver in human liver HepG2 and colon Caco2 cells evaluated by the cytokinesis block micronucleus assay. J. Appl. Toxicol. 36(4): 532-542.

Sandoval, B (2009). Perspectives on FDA's regulation of nanotechnology: emerging challenges and potential solutions. Compr. Rev. Food Sci. Food Saf. 8(4): 375-393.

Sastry, M., K.S. Mayyaa and K. Bandyopadhyay (1997). pH dependent changes in the optical properties of carboxylic acid derivatized silver colloid particles. Colloids Surf. A. 127(1-3): 221-228.

Savary, S., F. Andrea, J.N. Aubertot and C. Hollier (2012). Crop losses due to diseases and their implications for global food production losses and food security. Food Secur. 4(4): 519-537.

Shah, S., S. Dasgupta, M. Chakraborty, R. Vadakkekara, and M. Hajoori (2014). Green synthesis of iron nanoparticles using plant extracts. Int. J. Biol. Pharm. Res. 5(7): 549-552.

Shankar, S.S., A. Rai, A. Ahmad and M. Sastry (2004). Rapid synthesis of Au, Ag, and bimetallic Au core-Ag shell nanoparticles using Neem (*Azadirachta indica*) leaf broth. J. Coll. Inter. Sci. 275: 496-502.

Siddiqui, M.A., M.P. Kashyap, V. Kumar, A.A. Al-Khedhairy, J. Musarrat and A.B. Pant (2010). Protective potential of trans-resveratrol against 4-hydroxynonenal induced damage in PC12 cells. Toxicol. in Vitro. 24(6): 1592-1598.

Sinha, K., J. Ghosh and P.C. Sil (2017). New pesticides: A cutting-edge view of contributions from nanotechnology for the development of sustainable agricultural pest control A2—Grumezescu, Alexandru Mihai. In New Pesticides and Soil Sensors; Academic Press: Cambridge, MA, USA,:. [Google Schola

Srikar, S.K., D.D. Giri, D.B. Pal, P.K. Mishra and S.N. Upadhyay (2016). Green synthesis of silver nanoparticles: a review. Green Sustain. Chem. 6: 34-56.

Stroh, A., C. Zimmer, C. Gutzeit, M. Jakstadt, F. Marschinke, T. Jung, H. Pilgrimm and T. Grune (2004). Iron oxide particles for molecular magnetic resonance imaging cause transient oxidative stress in rat macrophages. Free Radical Biol. Med. 36(8): 976-984.

Sulaiman, G., A.A.W. Mohammada, H.E. Abdul-waheda and M.M. Ismailb (2013). Biosynthesis, antimicrobial and cytotoxic effects of silver nanoparticles using *Rosmarinus officinalis* extract. Dig. J. Nanomater. Bios. 8(1): 273-280.

Suman, T.Y., S.R. Rajasree, A. Kanchana and S.B. Elizabeth (2013). Biosynthesis, characterization and cytotoxic effect of plant mediated silver nanoparticles using *Morinda citrifolia* root extract. Colloids Surf. B 106: 74-78.

Vivek, R., R. Thangam, K. Muthuchelian, P. Gunasekaran, K. Kaveri and S. Kannan (2012). Green biosynthesis of silver nanoparticles from *Annona squamosa* leaf extract and its in vitro cytotoxic effect on MCF-7 cells. Process Biochem. 47(12): 2405-2410.

Wani, I.A., S. Khatoon, A. Ganguly, J. Ahmed, A.K. Ganguli and T. Ahmad (2010). Silver nanoparticles: large scale solvothermal synthesis and optical properties. Mater. Res. Bull. 45(8): 1033-1038.

Yesil-Celiktas, O., C. Sevimli., E.Bedir.,F. Vardar-Sukan (2010). Inhibitory Effects of Rosemary Extracts, Carnosic Acid and Rosmarinic Acid on the Growth of Various Human Cancer Cell Lines. Plant Foods Hum. Nutr. 65 (2), 158–163.

Zhao, J., A.O. Pinchuk, J.M. McMahon, S. Li, L.K. Ausman, A.L. Atkinson and G.C. Schatz (2008). Methods of describing the electromagnetic properties of silver and gold nanoparticles. Chem. Soc. Rev. 41(12): 1710-1720.